

1970

Strength of longitudinally stiffened plate girders under combined loads, December 1970 (71-45)

Alexis Ostapenko

Chingmiin Chern

Follow this and additional works at: <http://preserve.lehigh.edu/engr-civil-environmental-fritz-lab-reports>

Recommended Citation

Ostapenko, Alexis and Chern, Chingmiin, "Strength of longitudinally stiffened plate girders under combined loads, December 1970 (71-45)" (1970). *Fritz Laboratory Reports*. Paper 267.
<http://preserve.lehigh.edu/engr-civil-environmental-fritz-lab-reports/267>

This Technical Report is brought to you for free and open access by the Civil and Environmental Engineering at Lehigh Preserve. It has been accepted for inclusion in Fritz Laboratory Reports by an authorized administrator of Lehigh Preserve. For more information, please contact preserve@lehigh.edu.

589
LEHIGH UNIVERSITY



**OFFICE
OF
RESEARCH**

Unsymmetrical Plate Girders

**STRENGTH OF LONGITUDINALLY
STIFFENED PLATE GIRDERS
UNDER COMBINED LOADS**

FRITZ ENGINEERING
LABORATORY LIBRARY

by
**Alexis Ostapenko
and
Chingmiin Chern**

December 1970

Fritz Engineering Laboratory Report No. 328.10 C

Unsymmetrical Plate Girders

STRENGTH OF LONGITUDINALLY STIFFENED PLATE GIRDERS UNDER COMBINED LOADS

by

Alexis Ostapenko

and

Chingmiin Chern

This work was conducted as part of the project Unsymmetrical Plate Girders, sponsored by the American Iron and Steel Institute, the Pennsylvania Department of Transportation, the Federal Highway Administration of the U. S. Department of Transportation, and the Welding Research Council. The opinions, findings and conclusions expressed in this report are those of the authors and not necessarily those of the sponsors.

Department of Civil Engineering
Fritz Engineering Laboratory
Lehigh University
Bethlehem, Pennsylvania

December 1970

STRENGTH OF LONGITUDINALLY STIFFENED
PLATE GIRDERS UNDER COMBINED LOADS

by

Alexis Ostapenko¹

Chingmiin Chern²

ABSTRACT

A method is described for determining the static ultimate strength of longitudinally stiffened plate girder panels subjected to a combination of shear and bending. The method is applicable to symmetrical, unsymmetrical, homogeneous and hybrid girders. Compatibility of the deformations is maintained between the two web subpanels into which the web is subdivided by the longitudinal stiffener.

It is assumed that the ultimate strengths of the web plate subpanels and the plastic strength of the frame formed by the longitudinal stiffener, flanges and transverse stiffeners can be computed separately and that the ultimate strength of the whole panel is the sum of the strengths of these components. A continuous interaction relationship is obtained between shear and moment producing the ultimate condition of the girder panel. Comparison of the computed loads with available test results indicates that the proposed approach provides a reliable means for computing the ultimate strength of longitudinally stiffened plate girders.

¹Professor of Civil Engineering, Fritz Engineering Laboratory, Department of Civil Engineering, Lehigh University, Bethlehem, Pennsylvania.

²Assistant Professor of Civil Engineering, North Dakota State University, Fargo, North Dakota, formerly Research Assistant at Lehigh University, Bethlehem, Pa.

1. INTRODUCTION

Deep plate girders, to be economical, require the use of longitudinal stiffeners. The function of the stiffeners is to enforce the web to develop higher buckling strength and to carry additional forces after the web subpanels buckle.

As shown in Fig. 1, a girder panel is subdivided by the longitudinal stiffener into two subpanels, subpanels "1" and "0". The stiffener may be on one or both sides of the web and in most cases it is located closer to the compression flange in order to increase the bending buckling capacity of the web. Then, the narrow web subpanel "1" is subjected to shear and linearly varying compression stresses as shown in Fig. 2. The other subpanel (subpanel "0") is under shear and normal stresses varying linearly from compression to tension. For simplicity it is assumed here that the shear stress is constant across the girder depth rather than varying parabolically.

Most of the studies on longitudinally stiffened plate girders have dealt with the buckling strength of the stiffened web. (8,21,13, 16,18) Accordingly, design methods have also been based on the buckling strength as the limiting criterion. (1,3) Recognition of the fact that the web plate possesses considerable postbuckling capacity led to research on the ultimate strength. Particular emphasis was put on transversely stiffened plate girders, for example, Ref. 2.

A study was also performed on the ultimate static strength of longitudinally stiffened girders under shear or bending. (9) In shear, the web subpanels were assumed to develop their ultimate strength

independently from each other in the manner of transversely stiffened panels.

All of this research dealt with symmetrical girders, that is, the flanges were assumed to be of equal area with the result that the centroidal axis was at the mid-depth. Since many steel plate girders are unsymmetrical, the authors developed a new ultimate strength formulation for transversely stiffened girders. (5,6,7) This paper presents an extension of that formulation to longitudinally stiffened plate girders. Besides introducing a new analytical model for the individual subpanels, the method imposes a requirement on the compatibility of deformation between the subpanels. The result is a method which gives a continuous description of the plate girder strength under any combination of shear and moment.

The analytical model employed is still an approximation of the true behavior of a plate girder panel, but, in comparison with the available test data, it gives better and more consistent results than other proposed methods.

Panel Behavior

A web plate subpanel subjected to shear is shown in Fig. 3. Its stress-strain relationship is linear up to the point of buckling, τ_{cr} . Then, the shearing strain is

$$\gamma_{cr} = \frac{\tau_{cr}}{G} \quad (1)$$

As the shear force gradually increases beyond the web buckling load, the part of the shear in excess of the buckling value will be carried by the tension field action of the web. (5) The shear strain at the instant of reaching the ultimate load can be obtained approximately, although liberally, by considering the initiation of tensile yielding along the panel diagonal. According to Fig. 3, this shear strain is*

$$\gamma_u = \frac{\sigma_{yw}}{E} \left(\alpha + \frac{1}{\alpha} \right) \quad (2)$$

From here on the shear strain is assumed to increase at the same average shear stress as is to be expected in the plastic range. Although the transition from γ_{cr} to γ_u is generally non-linear and impossible to define exactly, for simplicity, it is assumed to be linear as shown, for example, by line AB in Fig. 4 for subpanel "0".

Application of Eqs. 1 and 2 to each subpanel individually and the compatibility requirement that the shear deformations in both subpanels be equal give a means of defining the shear-deformation response of the whole web panel. The panel behaves like an ordinary beam until subpanel "0" reaches its buckling stress τ_{co} , indicated by point A in Fig. 4. From then on, subpanel "0" develops tension field action which will produce additional shear deformation as illustrated by line AB in the figure. However, subpanel "1" will remain flat and continue behaving linearly until it reaches the buckling stress at point C. At this instant, subpanel "0" has not yet attained its ultimate strength since the compatibility relationship of the subpanels

*A more accurate formula is $\gamma_u = (1/E)(\sigma_{yw} - 0.7 \tau_{cr})(\alpha - 1/\alpha)$, but this or further refinements are hardly warranted.

indicates that $\gamma_{cl} < \gamma_{uo}$, that is, subpanel "1" will reach buckling state before subpanel "0" develops its ultimate strength. After subpanel "1" buckles, the subpanels develop their ultimate strengths individually.

When the shear force carried by the panel web is plotted as the ordinate instead of the average web shear stress, Fig. 4 is converted into Fig. 5. The web shear forces of the subpanels are obtained for this figure by assuming that the web shear force of subpanel "1" (shear stress multiplied by the web area of subpanel "1") is less than that of subpanel "0". After both subpanels reach their ultimate strengths, the web shear force curve becomes horizontal (line S-S').

When in addition to shear, bending stresses are acting on the subpanels as shown in Fig. 2, the web deformation pattern is analogous to those shown in Figs. 4 and 5 except that the critical buckling stresses τ_{co} and τ_{cl} are computed for a combined state of stress rather than for pure shear. It is assumed that the moment in excess of the moment which caused buckling of a subpanel web is carried only by the flanges, longitudinal stiffener and the unbuckled subpanel.

Stresses and forces that develop in the flanges and the longitudinal stiffener in the course of the deformation of the web panel may cause failure in one of them thus precipitating failure of the whole panel. The following modes of failure may be possible for a panel subjected to a combination of shear and bending: (a) shear failure of the web plate, (b) buckling or yielding of the compression flange, or (c) yielding of the tension flange. Failure of the longitudinal

stiffener by lateral or torsional buckling may precede (a), (b) and (c), but it will usually only reduce rather than limit the panel capacity by changing the panel in effect from a longitudinally stiffened to a transversely stiffened one.

The applicable mode is determined by calculating the stresses in the flanges and the longitudinal stiffener at each significant loading level and considering the inequality relationships of these reference stresses. This way an interaction curve is obtained. In the following, only the case is presented when the larger portion of the web is in compression. The strength of a girder panel with the larger portion of the web in tension can be obtained by a procedure similar to that described here.

Shear Span

For convenience, a girder panel subjected to a particular combination of shear and moment is visualized to be a panel in a girder shown in the top sketch of Fig. 6. The moment at the mid-panel can then be defined in terms of the shear span ratio μ .

$$\mu = \frac{M}{b V} = \frac{x - a/2}{b} \quad (3)$$

that is, $M = \mu b V$.

2. REFERENCE STRESSES

Stresses in the flanges, stiffener, and web subpanels are developed at various levels of loading by different mechanisms involving pre-buckling, post-buckling, and post-ultimate behavior of the individual panel components. The stresses at the transition from one mechanism to another are the reference stresses. Coupled with the requirement of compatibility, reference stresses provide a means of determining the mode of panel failure and the ultimate load. To simplify the explanation it is assumed in the following discussion that subpanel "1" is smaller than subpanel "0". However, the description and formulas can be readily modified for other relative proportions.

Stresses Due to the Load Causing Buckling of Subpanel "0"

The stresses at buckling of a rectangular panel fixed at the horizontal edges and pinned at the vertical edges^{*} and subjected to combined shear and bending (see Fig. 2) can be calculated with adequate accuracy by the following interaction equation: (5,11)

$$\left(\frac{\tau_{co}}{\tau_{cro}}\right)^2 + \frac{1 + R_o}{2} \left(\frac{\sigma_{bco}}{\sigma_{cpo}}\right) + \frac{1 - R_o}{2} \left(\frac{\sigma_{bco}}{\sigma_{cpo}}\right)^2 = 1.0 \quad (4)$$

where subscript "o" denotes subpanel "0" and

$$\tau_{co} = \text{shear stress at buckling under combined loads (a combination of shear and bending)}$$

$$\tau_{cro} = k_{vo} \frac{\pi^2 E}{12 (1 - \nu^2)} \left(\frac{1}{\beta_o}\right)^2, \text{ buckling stress under pure shear}$$

*This assumption of plate boundary conditions is justified by the results of a study conducted on this project.

with the shear buckling coefficient

$$k_{vo} = \frac{5.34}{\alpha_o^2} + \frac{6.55}{\alpha_o} - 13.71 + 14.10 \alpha_o \quad (5a)$$

for

$$\alpha_o < 1.0$$

or

$$k_{vo} = 8.98 + \frac{6.18}{\alpha_o^2} - \frac{2.88}{\alpha_o^3} \quad (5b)$$

for

$$\alpha_o \geq 1.0$$

$\sigma_{bco} =$ bending buckling stress under combined loads

$$\sigma_{cpo} = k_{bo} \frac{\pi^2 E}{12 (1 - \nu^2)} \left(\frac{1}{\beta_o} \right)^2 \quad \text{buckling stress at the extreme compression fiber of the subpanel under bending}$$

with the bending buckling coefficient k_{bo} taken at its minimum value

neglecting the effect of α_o (or setting $\alpha_o = \infty$)

$$k_{bo} = 13.54 - 15.64 R_o + 13.32 R_o^2 + 3.38 R_o^3 \quad (6)$$

valid for $-1.5 \leq R_o \leq 0.5$

$R_o =$ ratio of the maximum tensile stress (or minimum compressive stress) to the maximum compressive stress for subpanel "0" under combined loads as shown in Fig. 2

α_o and β_o are, respectively, the aspect ratio, $(a)/(b-b_1)$, and the slenderness ratio, $(b-b_1)/t$, of subpanel "0".

When subpanel "0" reaches the buckling stress τ_{co} , the total panel shearing force V_1 (Fig. 6) is given by

$$V_1 = \tau_{co} A_w \quad (7)$$

where

$$A_w = bt = \text{panel web area.}$$

Stress σ_{bco} at the web-to-longitudinal stiffener junction can be obtained according to the ordinary beam theory formula

$$\sigma_{bco} = \frac{V_1 (\mu b)}{I} (y_c - b_1) \quad (8)$$

where I is the moment of inertia of the girder cross section about the horizontal centroidal axis, y_c is the distance between the compression flange-web junction and the centroidal axis, and b_1 is the location of the longitudinal stiffener from the compression flange-web junction (Fig. 2).

The solution for V_1 is obtained by inserting τ_{co} and σ_{bco} expressed in terms of V_1 into Eq. 4

$$V_1 = \frac{\sqrt{p_2^2 + 4p_1} - p_2}{2p_1} \quad (9)$$

where

$$p_1 = \left(\frac{1}{A_w \tau_{cro}} \right)^2 + \frac{1 - R_o}{2} \left[\frac{(\mu b) (y_c - b_1)}{I \sigma_{cpo}} \right]^2$$

and

$$P_2 = \frac{1 + R_o}{2} \left[\frac{(\mu b) (y_c - b_1)}{I \sigma_{cpo}} \right]$$

With V_1 from Eq. 9, the shear buckling stress τ_{co} of subpanel "0" under combined loads can be calculated from Eq. 7. V_{TO} , the buckling strength contributed by subpanel "0" alone, is then

$$V_{TO} = \tau_{co} A_{wo} \quad (10)$$

where

$$A_{wo} = (b - b_1) t = \text{web area of subpanel "0"}$$

As shown in Fig. 6, the stresses in the compression flange and in the longitudinal stiffener are, respectively,

$$\sigma_{f1} = \frac{V_1 \mu b}{I} y_c \quad (11a)$$

and

$$\sigma_{l1} = \frac{V_1 \mu b}{I} (y_c - b_1) \quad (11b)$$

Stresses Due to the Load Causing Buckling of Subpanel "1"

Following the procedure described for panel "0" the buckling shear of subpanel "1" is calculated to be

$$V_{\tau 1} = \tau_{c1} A_{w1} \quad (12)$$

where τ_{c1} and A_{w1} are, respectively, the shear buckling stress and the web area of subpanel "1".

When $V_{\tau 1}$ is reached, the shear force carried by the whole panel web is

$$V_2 = V_{\tau 0} + V_{\tau 1} + V_{\sigma 0} \left(\frac{\gamma_{c1} - \gamma_{co}}{\gamma_{uo} - \gamma_{co}} \right) \quad (13)$$

where

$V_{\sigma 0} =$	shear strength of subpanel "0" when the tension field action is fully developed (Eq. 16)
$\gamma_{co} = \frac{\tau_{co}}{G}$	shear strain of subpanel "0" corresponding to the web buckling stress τ_{co}
$\gamma_{c1} = \frac{\tau_{c1}}{G}$	shear strain of subpanel "1" corresponding to the web buckling stress τ_{c1}
$\gamma_{uo} =$	approximate shear strain when subpanel "0" reaches its ultimate load; it is obtained from Eq. 2 by substituting α_o for α .

The increments of stresses in the compression flange and in the longitudinal stiffener, as shown in Fig. 7, in the interval of the panel shear from V_1 to V_2 are, respectively,

$$\sigma_{f2} = \frac{(V_2 - V_1) \mu b}{I} y_c \quad (14a)$$

and

$$\sigma_{\ell 2} = \frac{(V_2 - V_1) \mu b}{I} (y_c - b_1) + \frac{H'_o}{2A_{\ell s}} \quad (14b)$$

where H_o^1 is the horizontal component of the tension field force and is evenly split between the bottom flange and the longitudinal stiffener

$$H_o^1 = V_{\sigma\sigma} \frac{\gamma_{c1} - \gamma_{co}}{\gamma_{uo} - \gamma_{co}} \cot \phi_{co}$$

The compression flange stress σ_{f2} (Eq. 14a) is simply the bending stress. This is because subpanel "1" just reaches the buckling stage, and no post-buckling tension field force has yet developed in it. However, the longitudinal stiffener has to carry the horizontal component of the tension field force of subpanel "0" in addition to the stress contributed by the bending moment. This horizontal component of the yet not completely developed tension field force is given by Eq. 15a. (7)

Stresses Due to the Load Developing the Post-Buckling Strength of Subpanel "0"

In order to evaluate the tension field action strength of subpanel "0", a fictitious structure shown in Fig. 8 is employed. According to the discussion presented in the Introduction, subpanel "1" will buckle and then develop only its incomplete tension field action strength when subpanel "0" reaches its full tension field strength.

According to Ref. 7, the maximum tension field action contribution of subpanel "0" to the shear strength is

$$V_{\sigma o} = \frac{1}{2} \sigma_{to} A_{wo} \left[\sin 2\varphi_{co} - (1-\rho) \alpha_o + (1-\rho) \alpha_o \cos 2\varphi_{co} \right] \quad (16)$$

with σ_{to} from

$$\sigma_{to} = \sigma_{yw} (D_o + \sqrt{1 + B_o - C_o^2 + D_o^2}) \quad (17)$$

where

$$B_o = 3 \sqrt{C_o^2 + (\tau_{co}/\sigma_{yw})^2} \quad (18a)$$

$$C_o = -0.25 R_o (\sigma_{bco}/\sigma_{yw}) \quad (18b)$$

$$D_o = -0.5 \left\{ B_o \sin [\tan^{-1}(C_o \sigma_{yw}/\tau_{co}) + 2 \varphi_{co}] + C_o \right\} \quad (18c)$$

φ_{co} is the optimum inclination of the tension field of subpanel "0" under combined loads*, and ρ is the coefficient of the tension field stress in the elastic zone. ρ is assumed to be equal to 0.5 for conventional welded plate girders. In the above expressions subscript "o" denotes subpanel "0".

When subpanel "0" reaches its maximum capacity, the shear carried by the panel web will be

$$V_3 = V_{\tau o} + V_{\sigma o} + V_{\tau 1} + V_{\sigma 1} \left(\frac{\gamma_{uo} - \gamma_{cl}}{\gamma_{ul} - \gamma_{cl}} \right) \quad (19)$$

where

$V_{\sigma 1}$ = shear strength of subpanel "1" when the tension field action is fully developed (Eq. 21)

γ_{ul} = approximate shear strain when subpanel "1" reaches its ultimate load (Eq. 2 after substituting α_1 for α)

* φ_{co} is determined by optimizing $V_{\sigma o}$. (7)

When the panel shearing force is increased from V_2 to V_3 as shown in Fig. 8, the stresses added to the compression flange and to the longitudinal stiffener are, respectively,

$$\sigma_{f3} = \frac{(V_3 - V_2) \mu b}{I} y_c + \frac{H_1'}{2A_{fc}} \quad (20a)$$

and

$$\sigma_{l3} = \frac{(V_3 - V_2) \mu b (y_c - b_1)}{I} + \frac{H_1' + H_o''}{2A_{ls}} \quad (20b)$$

where

$$H_o'' = V_{\sigma o} \left[1 - \left(\frac{\gamma_{cl} - \gamma_{co}}{\gamma_{uo} - \gamma_{co}} \right) \right] \cot \varphi_{co} \quad (20c)$$

and

$$H_1' = V_{\sigma 1} \left(\frac{\gamma_{uo} - \gamma_{cl}}{\gamma_{ul} - \gamma_{cl}} \right) \cot \varphi_{cl} \quad (20d)$$

H_1' is the horizontal component of the tension field force of subpanel "1".

Stresses Due to the Load Developing the Post-Buckling Strength of Subpanel "1"

The tension field action contribution of subpanel "1", analogously to Eq. 16, is

$$V_{\sigma 1} = \frac{1}{2} \sigma_{t1} A_{w1} [\sin 2\varphi_{cl} - (1 - \rho) \alpha_1 + (1 - \rho) \alpha_1 \cos 2\varphi_{cl}] \quad (21)$$

with σ_{t1} from

$$\sigma_{t1} = \sigma_{yw} (D_1 + \sqrt{1 + B_1 - C_1^2 + D_1^2}) \quad (22)$$

where subscript "1" denotes subpanel "1". The only variable, which is different from those in Eq. 17, is

$$\begin{aligned} C_1 &= -0.25 R_1 (\sigma_{bc1} / \sigma_{yw}) \\ &= 0.25 \left(\frac{y_c - b_1}{y_c} \right) \left(\frac{\sigma_{f1} + \sigma_{f2}}{\sigma_{yw}} \right) \end{aligned} \quad (23)$$

As shown in Fig. 9, when subpanel "1" reaches its full tension field strength, the shear carried by the panel web will be the sum of the web strengths of the subpanels, that is,

$$V_4 = V_{\tau 0} + V_{\sigma 0} + V_{\tau 1} + V_{\sigma 1} \quad (24a)$$

or

$$V_4 = V_{u0} + V_{u1} \quad (24b)$$

where V_{u0} and V_{u1} are, respectively, the ultimate web strengths of web subpanels "0" and "1".

The increases in the compression flange stress and the longitudinal stiffener stress in the interval of shearing forces V_3 to V_4 are

$$\sigma_{f4} = \frac{(V_4 - V_3) \mu b}{I} y_c + \frac{H_1''}{2A_{fc}} \quad (25a)$$

and

$$\sigma_{\ell 4} = \frac{(V_4 - V_3) \mu b}{I} (y_c - b_1) + \frac{H_1''}{2A_{\ell s}} \quad (25b)$$

where

$$H_1'' = V_{\sigma 1} \left[1 - \left(\frac{\gamma_{uo} - \gamma_{c1}}{\gamma_{u1} - \gamma_{c1}} \right) \right] \cot \phi_{c1} \quad (25c)$$

The first terms of Eqs. 25a and 25b are due to the bending action of the increase in the shear force from V_3 to V_4 and the second terms are the reactions to the horizontal component of the tension field force in subpanel "1".

Stresses Due to Frame Action

The shear carrying capacity contributed by the strength of the flanges and the longitudinal stiffener is evaluated next. A structure consisting of the flanges and the longitudinal stiffener of a typical panel is shown in the upper portion of Fig. 10. It is assumed that the continuity of the web and flanges into the neighboring panels provides sufficient restraint to the transverse stiffeners so that they can perform as rigid supports for flanges and longitudinal stiffener of the panel under investigation. Then, the flanges and the longitudinal stiffener will behave like frame members resisting shear as plastic hinges form at both ends.

The shearing force V_f , contributed by the resulting plastic mechanism is

$$V_f = \frac{2}{a} (m_c + m_\ell + m_t) \quad (26)$$

where m_c , m_ℓ , and m_t are, respectively, the plastic moments of the compression flange, longitudinal stiffener, and the tension flange. The plastic moments are computed considering the axial forces in the members and are assumed to be equal at both ends of a member.*

The normal stresses in the flanges and stiffener are obtained by assuming that they are proportional to the distance from the centroidal axis of the cross section of the panel. Then, the normal stress on the stiffener is

$$\sigma_{\ell 5} = \sigma_{f5} \left(1 - \frac{b_1}{y_c} \right) \quad (27a)$$

The normal stress in the compression flange, σ_{f5} , is calculated by considering ~~the equilibrium of the horizontal forces and~~ the equilibrium of the moments acting on the cross section at the center of the panel,

$$\sigma_{f5} = \frac{\mu V_f}{A_{fc} + A_{\ell s} \left(1 - \frac{b_1}{y_c} \right) \left(1 - \frac{b_1}{b} \right)} \quad (27b)$$

Critical Stresses of the Compression Flange and Longitudinal Stiffener

The stability of the compression flange acting as a column is discussed in References 2,6,9 and 10. The function of the longitudinal stiffener is to enforce a nodal line in the deflected web at

*A refinement may consist of considering the plastic moments at the left and right ends of the panel separately. Then, $V_f = (1/a)(m_{cl} + m_{cr} + m_{\ell l} + m_{\ell r} + m_{tl} + m_{tr})$.

the theoretical web buckling load. Above the web buckling load, the stiffener should possess sufficient rigidity to control web deflections up to the ultimate load. According to Ref. 9, a convenient method of ensuring that this is the case is to consider the stability of the stiffener acting with a portion of the web as a column in a manner analogous to the compression flange column. (In the case of a one-sided stiffener, the beam-column analysis should be performed since the axial force will be applied eccentrically.) (17)

The slenderness parameters for the longitudinal stiffener column are given by

$$\lambda_{\ell} = a \sqrt{\frac{\epsilon_{ys} (A_{\ell s} + 20t^2)}{\pi^2 I_{\ell s}}} \quad (28a)$$

for lateral buckling of the stiffener column (Eq. 3.12 of Ref. 9), and

$$\lambda_t = \frac{c_s}{d_s} \sqrt{\frac{12 (1 - \nu^2) \epsilon_{ys}}{\pi^2 k_t}} \quad (28b)$$

for torsional buckling of the stiffener (Eq. 14a of Ref. 6),

where the additional notation is: ϵ_{ys} = yield strain of the longitudinal stiffener, $A_{\ell s}$ = area of the longitudinal stiffener = $2c_s \times d_s$ (for a two-sided stiffener), t = web thickness, $I_{\ell s}$ = moment of inertia of the longitudinal stiffener about the vertical axis of the panel, c_s = width of the longitudinal stiffener on each side, d_s = thickness of the longitudinal stiffener, and $k_t = 0.425$ is the torsional buckling coefficient.

Summary of Reference Stresses

- (a) The total stress introduced to the compression flange
when the subpanels reach their ultimate shear capacities

$$\sigma_{fs} = \sigma_{f1} + \sigma_{f2} + \sigma_{f3} + \sigma_{f4} + \sigma_{f5} \quad (29a)$$

- (b) The total stress introduced to the longitudinal stiffener
when the subpanels reach their ultimate shear capacities

$$\sigma_{ls} = \sigma_{l1} + \sigma_{l2} + \sigma_{l3} + \sigma_{l4} + \sigma_{l5} \quad (29b)$$

- (c) σ_{cf} = buckling stress of the compression flange column.

- (d) σ_{cl} = buckling stress of the longitudinal stiffener column.

3. ULTIMATE STRENGTH

Web or Compression Flange Failure

The two prevalent modes of failure of a longitudinally stiffened plate girder panel subjected to combined loads are the failure of the web plate or ^{the} buckling of the compression flange. Occurrence of one or the other depends on the relative values of the moment and shear.

The first mode is the shear type failure and it usually controls for combinations of high shear and low moment. For example, these combinations are designated by curve S_1-S_2 in Fig. 11 which gives a ^{continuous} ~~complete~~ non-dimensionalized plot of the ultimate combinations of shear and moment (interaction diagram). The non-dimensionalizing parameters are V_u , the ultimate shear for the case of pure shear, and M_u , the ultimate moment for the case of pure bending. The subpanels buckle and then develop their post-buckling strengths independently. When they reach their ultimate strengths, the total stresses introduced into the compression flange and into the longitudinal stiffener due to bending and the horizontal components of the tension field force are both less than the critical values.

The panel capacity expressed by means of the shear force V_{th} is obtained by adding up the shears from Eqs. 24b and 26.

$$V_{th} = V_{uo} + V_{ul} + V_f \quad (30a)$$

The final form of V_{th} is obtained by introducing Eqs. 10, 12, 16, 21, and 26 into Eq. 30a

$$\begin{aligned}
V_{th} = & \tau_{co} A_{wo} + \frac{1}{2} \sigma_{to} A_{wo} [\sin 2\varphi_{co} - (1-\rho) \alpha_o + (1-\rho) \alpha_o \cos 2\varphi_{co}] \\
& + \tau_{cl} A_{wl} + \frac{1}{2} \sigma_{tl} A_{wl} [\sin 2\varphi_{cl} - (1-\rho) \alpha_1 + (1-\rho) \alpha_1 \cos 2\varphi_{cl}] \\
& + \frac{2}{a} (m_c + m_\ell + m_t)
\end{aligned} \tag{30b}$$

The corresponding moment acting at the center of the panel is

$$M_{th} = V_{th} \mu b \tag{30c}$$

When the panel is subjected to high moment, the subpanel webs will not be able to develop their full capacities because the stresses introduced to the compression flange by the full tension field action of the subpanels would be greater than the buckling stress of the compression flange column. Thus, the mode of failure is classified as the flange failure and the corresponding portion in the interaction curve is represented in Fig. 11 by S_2 to S_3 .

In many cases, the aspect ratio of subpanel "1" is greater than 3.0. According to the results of the study in Refs. 4, 5 and 7, the ultimate strength of a girder panel in this case is suggested to be the sum of the strength contributed by the web buckling and by the flange strength. Thus, the stress in the compression flange will be the flexural stress only. Then, the interaction curve is represented by the two curve portions $S_1-S'_2$ and S'_2-S_3 in Fig. 11. With the maximum moment capacity that the compression flange can resist given by

$$M_{th} = \frac{\sigma_{cf} I}{y_c} \tag{31a}$$

the shear force at the mid-length of the panel for S_2-S_3 is

$$V_{th} = \frac{M_{th}}{\mu b} \quad (31b)$$

Tension Flange Yielding

Depending on the location of the centroidal axis it is also possible that yielding of the tension flange may precede the types of failure described above. The total stress in the tension flange due to various effects can be obtained in a manner analogous to that for the stress in the compression flange; the σ -sketches in Figs. 6 to 10 illustrate the individual contributions.

Maximum Moment in Panel

Since under combined loads the moment at one end of the panel is greater than the mid-panel moment which is used in the analysis, it may happen that this maximum panel moment will control the panel strength. This is especially true for panels with large aspect ratios. The shear producing the maximum panel moment may not exceed

$$V_{th}' \leq \frac{M_u}{b (\mu + \frac{1}{2} \alpha)} \left(\frac{\sigma_{yc}}{\sigma_{cf}} \right) \quad (32a)$$

It seems also reasonable and sufficiently accurate, mostly on the safe side, to keep the maximum panel moment below the moment which would produce yielding according to the ordinary beam theory. Then

$$V_{th}' \leq \frac{I \sigma_{yf}}{y b (\mu + \frac{1}{2} \alpha)} \quad (32b)$$

where σ_{yf} is the yield stress and y is the distance from the centroid to the compression or tension flange, whichever gives the smaller V_{th}' and thus controls.

Panels with Inadequate Longitudinal Stiffener

When the longitudinal stiffener subjected to the compressive force due to bending and the horizontal components of the tension field forces buckles laterally or torsionally before the panel develops its strength in one of the modes described above, the ultimate capacity of the panel will be reached in a different mechanism than discussed above.

The true failure mechanism in this case is too complicated to be analyzed at present; it would involve, for example, consideration of the post-buckling behavior of the longitudinal stiffener and of the rearrangement of the two-subpanel tension field pattern into a one-panel tension field. Two simplified and conservative limits of the ultimate strength are suggested here: (a) the panel develops its ultimate strength as if it had no longitudinal stiffeners --- the interaction diagram is indicated schematically by curve $Q_1 - Q_2 - Q_3$ in Fig. 12; or (b) the longitudinal stiffener column fails and the ultimate strength of the panel is considered to be limited by the strength attained at this point --- this case is given by curve $T_1 - T_2 - T_3$ in Fig. 12. Depending on the proportions of the panel and the relative magnitudes of the moment and shear, one or the other limit will give a higher value which is then to be taken as the ultimate load. The schematic plot of Fig. 12

gives the strength controlled by the longitudinal stiffener; however, the plots in Fig. 17 for particular panels show the controlling mode to be dependent on the moment-shear ratio. Of course, the true ultimate load should lie above the two modes discussed.

The ultimate strength for case (a), when the panel fails as if it had no longitudinal stiffener, is determined according to Reference 7.

When the panel strength is limited by the premature buckling of the longitudinal stiffener, the capacity expressed in terms of the shear strength is given by

$$V_{th} = V_{\tau 0} + V'_{\sigma 0} + V_{\tau 1} + V'_{\sigma 1} + V_f \quad (33)$$

where: V_f is computed from Eq. 26, $V_{\tau 1}$ - from Eq. 12, $V_{\tau 0}$ - from Eq. 10, $V'_{\sigma 1}$ is the incomplete tension field shear strength contributed by subpanel "1" at the point when the longitudinal stiffener reaches its buckling stress and $V'_{\sigma 0}$ is the incomplete tension field shear strength contributed by subpanel "0" at the point when the longitudinal stiffener reaches its buckling stress.

$V'_{\sigma 0}$ is given by

$$V'_{\sigma 0} = \frac{2 A_{\ell s} [\sigma_{cl} - \sigma_{\ell 5} - \frac{(V_{\tau 0} + V_{\tau 1} + V'_{\sigma 1}) \mu b}{I} (y_c - b_1)] - V'_{\sigma 1} \cot \phi_{c1}}{2 \frac{A_{\ell s} \mu b}{I} (y_c - b_1) + \cot \phi_{co}} \quad (34)$$

Since for essentially all practical girders $\alpha_1 > 3.0$, it is recommended to use $V'_{\sigma 1} = 0$ in Eq. 34. (Otherwise, an equation for $V'_{\sigma 1}$ can be derived on the basis of Figs. 4 and 5.)

4. COMPARISON WITH TEST RESULTS

The method of analysis developed in this paper is compared with available test results in Tables 1 and 2. Included are the tests that could be found in literature and had enough data to be analyzed. (9, 17, 20) The average deviation of the nineteen tests is 5% with the maximum deviation of 14%.

The results of six tests on symmetrical girder panels which failed under the combination of high shear and relatively low moment (Ref. 9) are shown graphically in Figs. 13 and 14. The mode of failure is classified as the web failure and the average deviation of the theory is 4% with a maximum of 8%.

Six tests on unsymmetrical girder panels were described in Ref. 20 and are shown in Figs. 15 and 16. Two end panels, UG5.1 and UG5.6, were subjected primarily to high shear and failed in the web. Four ~~specimens,~~ ~~tests,~~ UG5.2 to 5.5, were subjected to a combination of high shear and high moment. An average deviation of 5% is obtained for these tests with the extreme deviation of 12% (UG5.6).

F11-T1 of Ref. 17 was primarily subjected to high shear. Since the buckling strength of the longitudinal stiffener was not enough to generate the full web strength of the subpanels, the mode of failure is classified as that of a panel with inadequate longitudinal stiffener. The corresponding location on the interaction curve is either on $T_1 - T_2 - T_3$ or on $Q_1 - Q_2 - Q_3$ of Fig. 12, whichever is higher. The interaction curves of F11-T1, evaluated as the panel strength limited by the

strength of the longitudinal stiffener or as the strength obtained by neglecting the longitudinal stiffener, are plotted in Fig. 17*. The deviation of the test result is 3% from the ultimate strength obtained neglecting the longitudinal stiffener.

The theoretical load of F11-T2 was limited by the strength of the longitudinal stiffener column. The interaction curve and the test result are shown in Fig. 17. A 14% underestimate is obtained.

The predicted load of F11-T3 was obtained by the same procedure as for F11-T1 (Fig. 17 and Table 1). The test was terminated due to a failure outside the test panel and thus no valid comparison between the theory and test can be made.

The light dashed lines in Fig. 17 show the approximate interaction curves for the three panels if the longitudinal stiffeners were adequate.

A comparison of the ultimate strengths of two girder panels, one with and the other without a longitudinal stiffener, is shown in Fig. 18. Three plots are made from the data in Ref. 20. In each case, panel dimensions and the type of loading were identical. UG4.1 and UG5.1 were subjected to high shear and relatively low moment and are classified as the web failure mechanisms, and the introduction of the longitudinal stiffener lead to an increase in the panel strength of about 13%. On the other hand, UG4.3 and UG5.3, or UG4.4 and UG5.4, were subjected to a combination of high shear and high moment. The panel capacity was limited by the flange strength, and the increase in the strength due to the contribution of the longitudinal stiffener was approximately 44%. This fact indicates that considerable economic advantage can be achieved

* V_u and M_u in Fig. 17 designate the theoretical ultimate shear and moment of the panel without the longitudinal stiffener.

by introducing a longitudinal stiffener to panels with smaller flange in compression and subjected to high shear and high moment.

Panels subjected to pure bending are shown in Table 2. A good correlation is obtained for these tests.

5. SUMMARY AND CONCLUSIONS

The following conclusions can be drawn from this investigation on the ultimate strength of longitudinally stiffened plate girder panels subjected to a combination of shear and moment:

- 1) The interaction curve between the ultimate values of moment and shear consists of two portions: web failure which occurs under dominant shear and flange failure which occurs under dominant moment.
- 2) The panel strength for the web failure mode may be assumed to be a sum of the ultimate shear strengths of the individual web subpanels (buckling and post-buckling strengths) and the capacity of the plastic mechanism formed by the flanges and longitudinal stiffener (frame action). A moment reduces the buckling and post-buckling ~~strengths~~ ^{contributions} of the web subpanels and the plastic hinges in the frame.
- 3) The force in a flange for the flange failure mode has contributions from the bending moment, redistribution of the stress from the web after web buckling and a component of the force from the partially developed tension field.
- 4) When the longitudinal stiffener is inadequate, the failure load may be conservatively assumed to be the higher one of the following:
(a) the ultimate strength of the panel as if it had no longitudinal stiffener or (b) the strength developed by the panel at the point when the longitudinal stiffener column fails.
- 5) A comparison of the theory with the results of fifteen tests on panels under combined loads and four panels under pure bending gives an average correlation of 5% with an extreme deviation of 14% (for

a panel with an inadequate stiffener). Thus, it may be concluded that the theory presented provides a reliable means of determining the static ultimate strength of longitudinally stiffened steel plate girder panels subjected to shear, bending or a combination of shear and bending.

- 6) One of the important factors contributing to the good accuracy of the method is believed to be the assumption that the web plate is fixed rather than simply supported at the flanges and the longitudinal stiffener.
- 7) Introduction of a longitudinal stiffener was found to increase the girder strength under a combination of shear and moment to substantially greater degree than under pure shear or pure moment.
- 8) In application, the method involves some lengthy iterative operations and, thus, it is hardly suitable for manual calculations. However, simple design formulas can be developed from the numerical computer output of a program based on the presented method. This work is suggested as an area for future research.

6. ACKNOWLEDGEMENTS

This paper was prepared as part of a research project on unsymmetrical plate girders conducted in the Department of Civil Engineering, Fritz Engineering Laboratory, Lehigh University, Bethlehem.

The authors are grateful to the sponsors of this project: Welding Research Council, American Iron and Steel Institute, Pennsylvania Department of Transportation, and Federal Highway Administration of the U. S. Department of Transportation. They also gratefully acknowledge the technical guidance provided by the Welded Plate Girder Subcommittee of Welding Research Council under the consecutive chairmanship of Mr. M. Deuterman, E. G. Paulet, and G. F. Fox and by the Task Group on Unsymmetrical Plate Girders under the chairmanship of Mr. C. A. Zwissler and, lately, Mr. L. H. Daniels.

The detailed review of the report made by Messrs. H.G. Juhl and J. Nishanian, respectively, of the Pennsylvania Department of Transportation and the Federal Highway Administration is sincerely appreciated.

Appreciation is due to Misses S. Matlock and K. Philbin for typing and Mr. J. M. Gera for drafting.

7. APPENDIX I. - REFERENCES

1. American Association of State Highway Officials
STANDARD SPECIFICATIONS FOR HIGHWAY BRIDGES, 1969.
2. Basler, K. and Thurlimann, B.
STRENGTH OF PLATE GIRDERS IN BENDING, J. ASCE, Vol. 87
(ST6), August, 1961.
3. British Standards Institution
STEEL GIRDER BRIDGES, British Standard 153,
Part 3B and 4, 1958.
4. Carskaddan, P. S.
SHEAR BUCKLING OF UNSTIFFENED HYBRID BEAMS,
J. ASCE, Vol. 94 (ST8), Aug., 1968.
5. Chern, C., and Ostapenko, A.
ULTIMATE STRENGTH OF PLATE GIRDERS UNDER SHEAR,
Fritz Engineering Laboratory Report No. 328.7,
Lehigh University, Aug., 1969.
6. Chern, C., and Ostapenko, A.
BENDING STRENGTH OF UNSYMMETRICAL PLATE GIRDERS,
Fritz Engineering Laboratory Report No. 328.8,
Lehigh University, Sept., 1970.
7. Chern, C., and Ostapenko, A.
UNSYMMETRICAL PLATE GIRDERS UNDER SHEAR AND MOMENT,
Fritz Engineering Laboratory Report No. 328.9,
Lehigh University, Oct., 1970.
8. Cooper, P. B.
LITERATURE SURVEY ON LONGITUDINALLY STIFFENED PLATES,
Fritz Engineering Laboratory Report No. 304.2,
Lehigh University, Sept., 1965.
9. Cooper, P. B.
BENDING AND SHEAR STRENGTH OF LONGITUDINALLY STIFFENED
PLATE GIRDERS, Fritz Engineering Laboratory Report No.
304.6, Lehigh University, Sept., 1965.
10. Johnston, B. G., Editor
DESIGN CRITERIA FOR METAL COMPRESSION MEMBERS,
Second Edition, John Wiley & Sons, Inc., 1966.
11. Kollbrunner, C. F., and Meister, M.
AUSBEULEN, Springer-Verlag, Berlin, 1958.

12. Lew, H. S., and Toprac, A. A.
THE STATIC STRENGTH OF HYBRID PLATE GIRDERS,
Structural Fatigue Research Laboratory, Dept. of
Civil Engineering, The University of Texas, Austin,
Texas, January, 1968.
13. Massonnet, C., Mazy, G., and Tanghe, A.
GENERAL THEORY OF THE BUCKLING OF ORTHOTROPIC
RECTANGULAR PLATES, CLAMPED OR FREELY SUPPORTED
AT THE EDGES, PROVIDED WITH STIFFENERS, PARALLEL
TO THE EDGES, HAVING CONSIDERABLE FLEXURAL AND
TORSIONAL RIGIDITY, Pub. IABSE, Vol. 21, 1960.
14. Ostapenko, A.
LOCAL BUCKLING, Chapter 17, STRUCTURAL STEEL DESIGN,
The Ronald Press Co., New York, 1964.
- ~~15. Ostapenko, A., and Dimitri, J. R.
BUCKLING OF PLATE GIRDER WEBS,
Fritz Engineering Laboratory Report No. 328.3,
Lehigh University, (in preparation).~~
16. Owen, D. R. J., Rockey, K. C., and Skaloud, M.
BEHAVIOR OF LONGITUDINALLY REINFORCED PLATE GIRDERS,
Final Report of the Eighth Congress of the International
Association for Bridges and Structural Engineering,
Theme IIc, Sept., 1968.
17. Patterson, P. J., Corrado, J. A., Huang, J. S., and Yen, B. T.
FATIGUE AND STATIC TESTS OF TWO WELDED PLATE GIRDERS,
WRC Bulletin 155, New York, October, 1970
18. Rockey, K. C.
BUCKLING UNDER PURE BENDING OF STIFFENED WEB PLATES-
SINGLE LONGITUDINAL STIFFENER HAVING BOTH TORSIONAL
AND FLEXURAL STRENGTH, American Institute of Steel
Construction, Inc., 1961.
19. Rockey, K. C.
SHEAR BUCKLING OF A WEB REINFORCED BY VERTICAL
STIFFENERS AND A CENTRAL HORIZONTAL STIFFENER,
Publication IABSE, Vol. 17, 1957.
20. Schueller, W., and Ostapenko, A.
TESTS ON A TRANSVERSELY STIFFENED AND ON A LONGITUDINALLY
STIFFENED UNSYMMETRICAL PLATE GIRDER, WRC Bulletin 156,
New York, November, 1970.
21. Timoshenko, S. P.
ÜBER DIE STABILITÄT VERSTEIFTER PLATTEN, Eisenbau,
Vol. 12, 1921.

8. APPENDIX II. - NOTATION

In general, subscripts "l" and "o" refer to subpanels "1" and "0", respectively. Subscript "ex" means experimental, "y" - yielding, "u" - ultimate.

1) Lower Case Letters

a	Panel length.
b	Panel depth (in Fig. 3, width of plate).
b_l	Depth of subpanel "1".
c_c	Half width of the compression flange.
c_s	Width of the longitudinal stiffener.
c_t	Half width of the tension flange.
d_c	Thickness of the compression flange.
d_s	Thickness of the longitudinal stiffener.
d_t	Thickness of the tension flange.
k_b	Plate buckling coefficient for pure bending.
k_t	Torsion buckling coefficient, 0.425.
k_v	Plate buckling coefficient for pure shear.
m_c, m_ℓ, m_t	Plastic moments in the compression flange, longitudinal stiffener and tension flange in frame action.
p_1, p_2	Parameters, used in Eq. 9.
t	Web plate thickness.
y_c	Distance from the neutral axis to the extreme compression fiber of the web panel before buckling.
y_t	Distance from the neutral axis to the extreme tension fiber before buckling.

2) Upper Case Letters

A_{fc}	Area of the compression flange.
A_{ft}	Area of the tension flange.
A_{ls}	Area of the longitudinal stiffener.
A_w	Area of the web.
$\left. \begin{array}{l} B \\ C \\ D \end{array} \right\}$	Parameters used in Eq. 17 and defined in Eqs. 18a,b,c.
E	Modulus of elasticity; for steel, 29,600 ksi.
G	Shear modulus.
H	Horizontal component of the tension field force; H' for the incomplete tension field.
I	Moment of inertia of the girder cross section.
I_{ls}	Moment of inertia of the longitudinal stiffener.
L	Laterally unsupported length of the compression flange.
M	Moment acting at mid-length of the panel.
M_{th}	Theoretical ultimate moment of the girder panel under combined loads.
M_u	Ultimate moment of the girder panel under pure bending.
R	Ratio of the maximum tensile stress (or minimum compressive stress) to the maximum compressive stress of the web plate panel (or subpanel). Note that R is negative when the stress is tensile.
V	Shear force.
V_1, V_2, V_3, V_4	Shear force in the web plate at various stages of loading.
V_f	Frame action shear.
V_p	Plastic shear of the web plate.
V_{th}	Theoretical ultimate shear strength of the plate girder panel.
V'_{th}	Limiting shear for the maximum moment in the panel.

V_u	Theoretical ultimate shear strength of the girder panel under pure shear.
V_{ul}, V_{uo}	Ultimate shear strengths of subpanel webs "1" and "0" under combined loads.
V_σ	Shear due to tension field action; V'_σ , for the incomplete tension field.
V_τ	Shear due to beam action at the moment of buckling of the web plate.

3) Greek Letters

$\alpha = a/b$	Aspect ratio, that is, length to depth ratio of the web plate; α_1 and α_0 , for subpanels.
$\beta = b/t$	Web slenderness ratio, that is, depth to thickness ratio of the web plate; β_1 and β_0 , for subpanels.
γ	Shearing strain.
γ_u	Approximate shear when the web plate panel (or subpanel) reaches its ultimate capacity.
ϵ_{ys}	Yield strain of the longitudinal stiffener.
$\mu = M/bV$	Shear span ratio.
ν	Poisson's ratio; 0.3 for steel.
ρ	Averaging coefficient of the tension field stress in the elastic triangular portions; assumed 0.5 for ordinary welded steel girders.
σ_{bc}	Bending buckling stress under combined loads in the web.
σ_{cf}	Buckling stress of the compression flange column.
σ_{cl}	Buckling stress of the longitudinal stiffener column.
σ_{cp}	Theoretical buckling stress of the web plate under bending only.
σ_f	Stress in the compression flange.
σ_{fs}	Total stress in the compression flange.
σ_{ls}	Total stress in the longitudinal stiffener.
σ_t	Tension field stress in the fully yielded zone.

σ_{yc}	Yield stress of the compression flange.
σ_{ys}	Yield stress of the longitudinal stiffener.
σ_{yt}	Yield stress of the tension flange.
σ_{yw}	Yield stress of the web plate.
τ	Shearing stress.
τ_c	Shearing buckling stress under combined loads.
τ_{cr}	Theoretical shearing buckling stress under pure shear.
φ_c	Optimum inclination of the tension field force.
α	Ratio of the horizontal to vertical component of the tension field force.

9. TABLES AND FIGURES

Table 1. Tests on Longitudinally Stiffened Plate Girders Under Shear and Bending

Source	Test No.	α	β	Web		Comp. Flange		Tens. Flange		Longit. Stiffener			L in	$\mu = \frac{M}{Vb}$	V_{ex} kip	V_{th} kip	$\frac{V_{ex}}{V_{th}}$
				b x t	σ_{yw}	$2c_c \times d_c$	σ_{yc}	$2c_t \times d_t$	σ_{yt}	$c_s \times d_s$	σ_{ys}	b_l					
				in x in	ksi	in x in	ksi	in x in	ksi	in x in	ksi	in					
1	2	3	4	5	6	7	8	9	10	11	12	13	14	15	16	17	18
Ref.9	LS1-T2	1.0	256	50x.195	46.8	14.12x1.498	30.5	14.10x1.497	30.5	4.04x1.016	30.6	16.5	75	2.5	207	207	1.00
	LS2-T1	1.0	275	50x.182	39.4	14x12x1.494	30.0	14.12x1.503	30.0	3.97x0.500	39.8	16.5	"	2.5	158	168	0.94
	LS3-T1	1.5	276	50x.181	38.2	14.24x1.516	29.8	14.20x1.516	29.8	1.97x0.502	39.2	16.5	"	0.75	139	138	1.01
	LS3-T2	1.5	"	"	"	"	"	"	"	3.44x0.511	"	"	"	2.25	148	148	1.00
	LS3-T3	0.75	"	"	"	"	"	"	"	3.44x0.511	"	"	"	2.63	169	183	0.93
	LS4-T1	1.0	260	50x.192	48.6	14.12x1.511	30.5	14.22x1.508	30.5	3.50x0.511	36.3	10.0	"	2.5	190	175	1.08
Ref.20	UG5.1	1.77	400	48x.120	56.2	10.00x0.750	33.4	13.00x1.375	33.4	3.00x0.750 3.00x0.750	33.4	12.5	85	1.01	97	92	1.06
	UG5.2	1.15	"	"	"	"	"	"	"	"	"	"	55	2.47	118	110	1.06
	UG5.3	1.46	"	"	"	"	"	"	"	"	"	"	70	3.77	93	96	0.97
	UG5.4	1.77	264	48x.182	34.3	"	"	"	"	"	"	"	85	1.01	97	97	1.00
	UG5.5	0.83	"	"	"	"	"	"	"	"	"	"	40	2.31	137	143	0.96
	UG5.6	1.77	"	"	"	"	"	"	"	"	"	"	85	1.01	109	124	0.88
Ref.17	F11-T1	1.39	365	95x.260	34.2	14.16x1.259	24.7	14.16x1.259	24.7	4.50x0.500	34.2	19.0	132	0.89	266	258	1.03
	F11-T2	1.20	"	"	34.2	"	24.7	"	"	"	"	"	114	1.79	247	216	1.14
	F11-T3	1.00	"	"	34.2	"	24.7	"	"	"	"	"	95	0.69	279	297	0.94

Table 2. Tests on Longitudinally Stiffened Plate Girders Under Bending

Source	Test No.	α	β	Web		Comp. Flange		Tens. Flange		Longi. Stiffener			L in	M_{ex} k-ft	M_u k-ft	$\frac{M_{ex}}{M_u}$
				b x t	σ_{yw}	$2c_c \times d_c$	σ_{yc}	$2c_t \times d_t$	σ_{yt}	$c_s \times d_s$	σ_{ys}	b_l				
				in x in	ksi	in x in	ksi	in x in	ksi	in x in	ksi	in				
1	2	3	4	5	6	7	8	9	10	11	12	13	14	15	16	17
Ref. 9	LB2	1.00	447	55x.123	34.1	12x.75	37.0	12x.75	37.1	2.0x.123	34.1	11	55	1520	1536	0.99
	LB3	1.00	"	"	34.5	"	36.0	"	36.1	2.5x.123	34.5	"	55	1500	1499	1.00
	LB4	1.50	"	"	35.8	"	34.9	"	35.5	2.0x.123	35.6	"	41	1470	1436	1.02
	LB5	0.75	"	"	35.6	"	35.3	"	35.5	2.0x.123	35.6	"	41	1508	1483	1.02

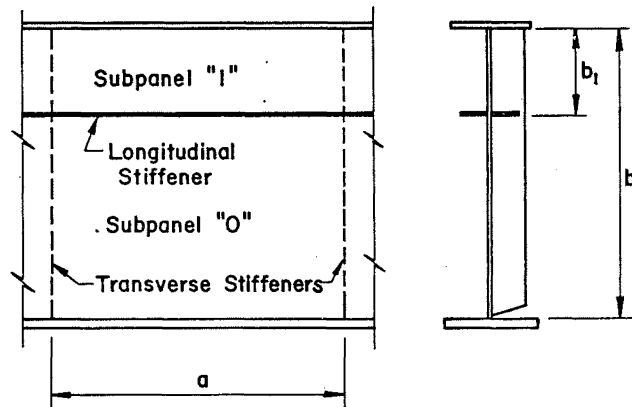


Fig. 1 Longitudinally Stiffened Girder Panel

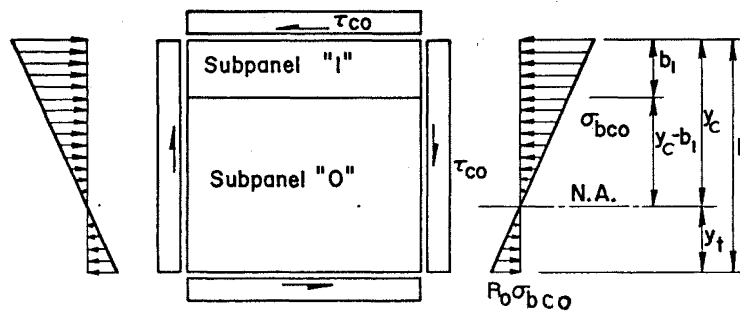


Fig. 2 Stresses at Buckling Load of Subpanel "O"

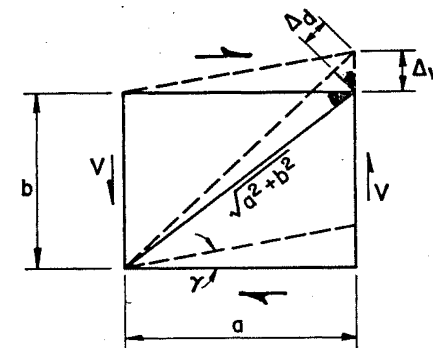


Fig. 3 Shear Deformation Diagram

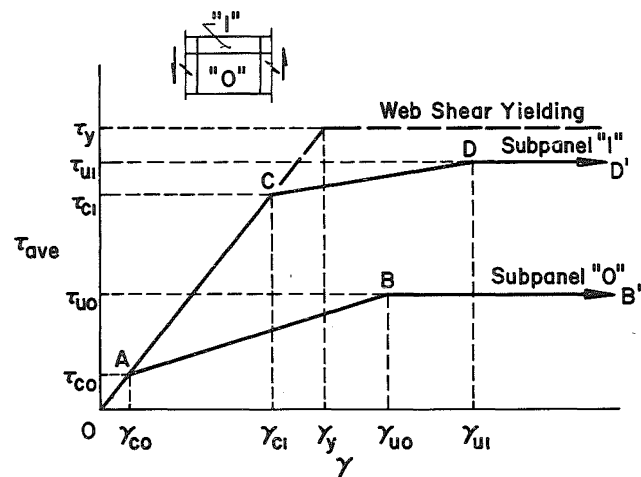


Fig. 4 Schematic Shear Stress - Strain Curve of a Longitudinally Stiffened Girder Panel

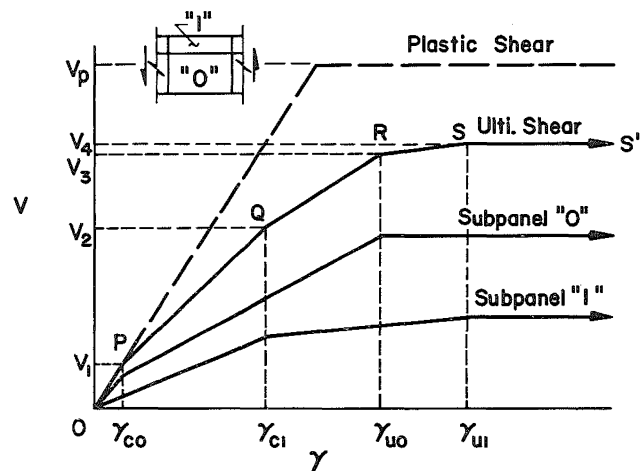


Fig. 5 Schematic Shearing Force - Strain Curve of a Longitudinally Stiffened Girder Panel

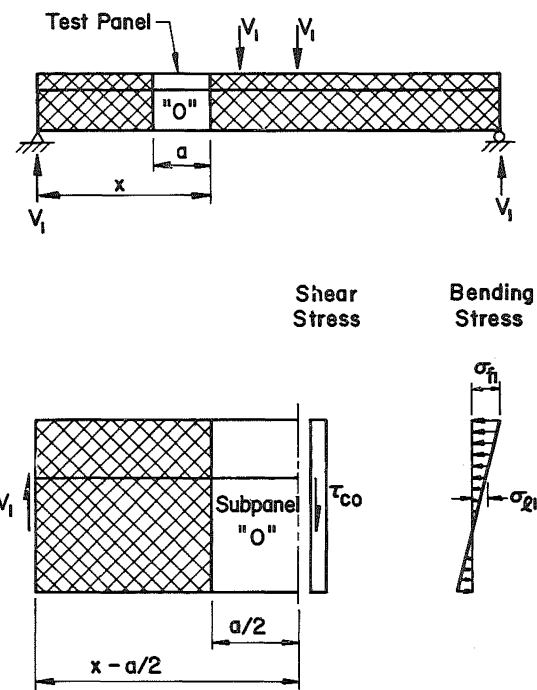
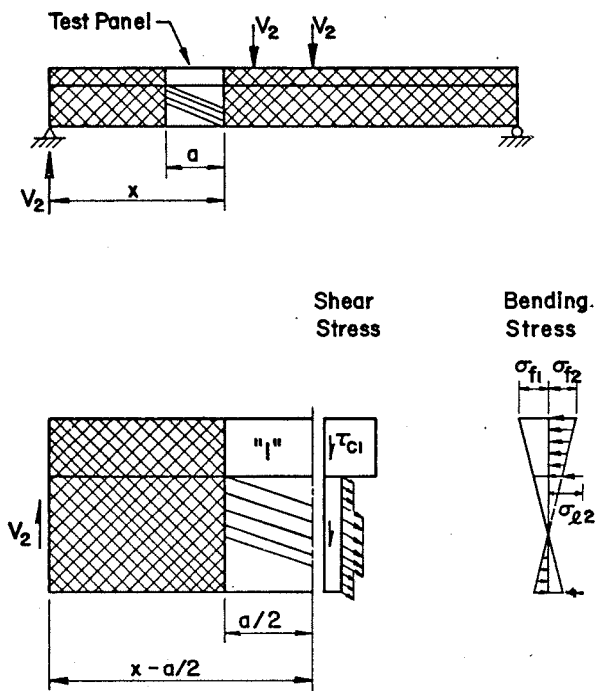
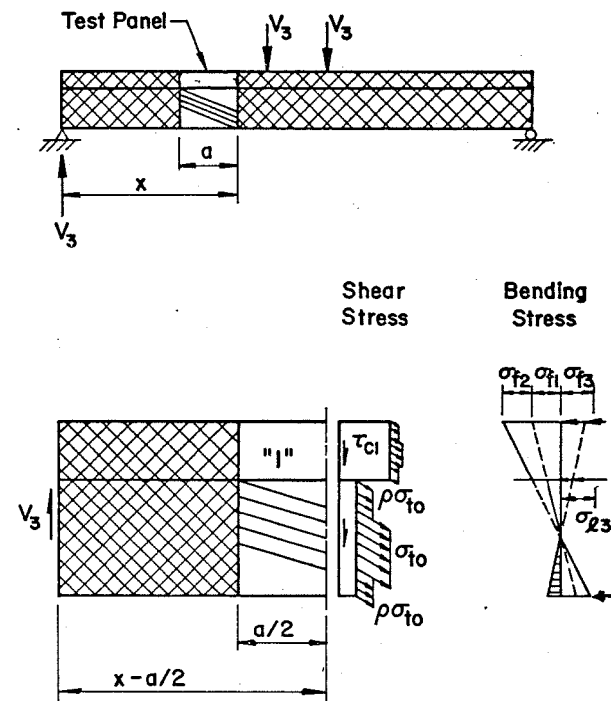


Fig. 6 Reference Stresses σ_{fl} & σ_{el}

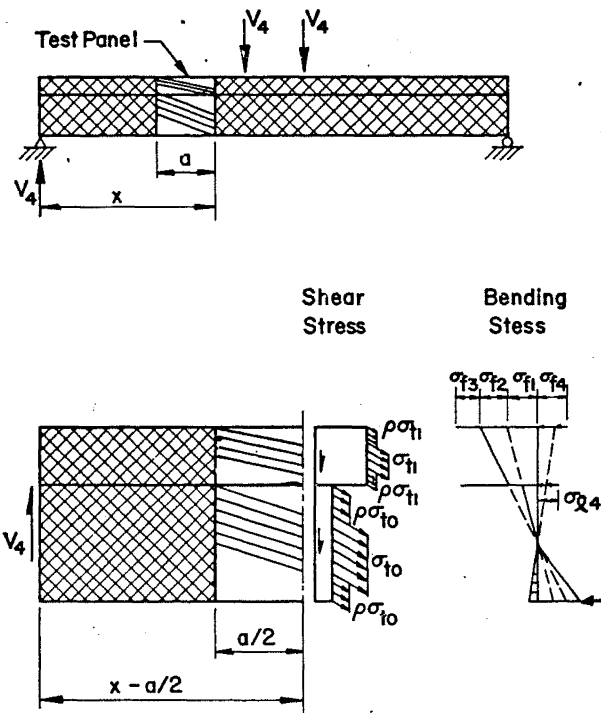
328.10

Fig. 7 Reference Stresses σ_{f2} & σ_{l2}

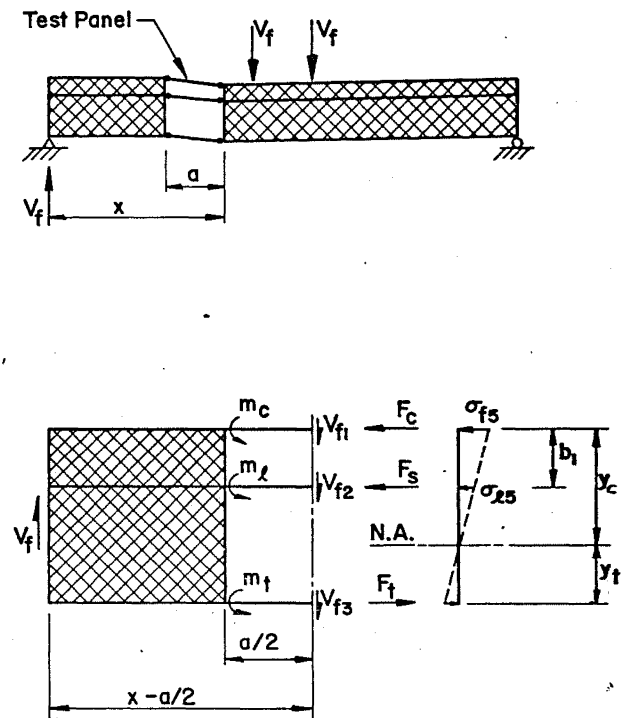
328.10

Fig. 8 Reference Stresses σ_{f3} & σ_{l3}

328.10

Fig. 9 Reference Stresses σ_{f4} & σ_{t4}

328.10

Fig. 10 Reference Stresses σ_{f5} & σ_{t5}

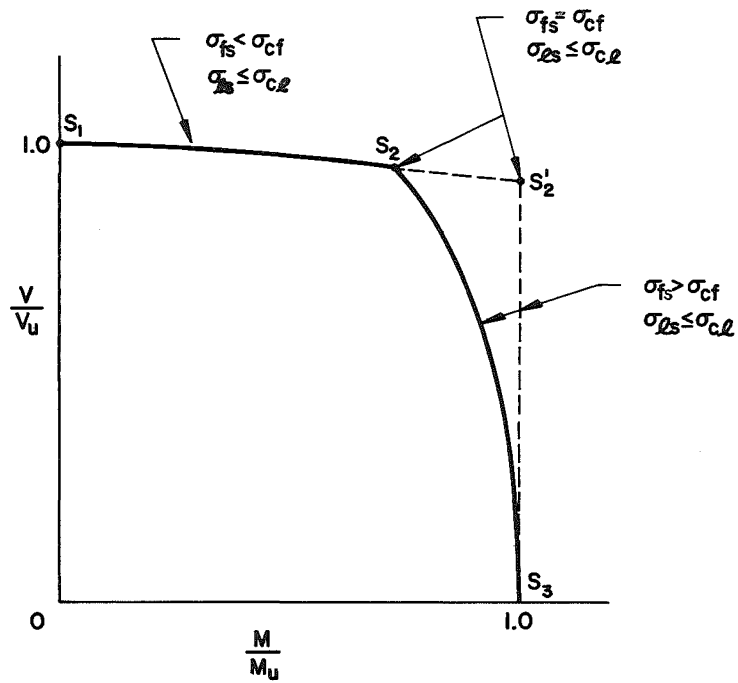


Fig. 11. Schematic Interaction Curve of a Panel with Adequate Longitudinal Stiffener

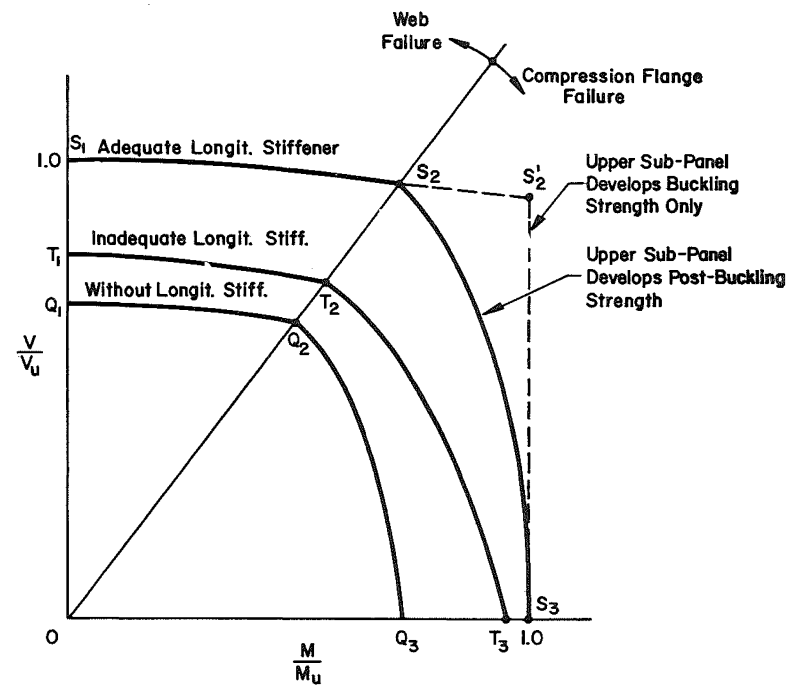
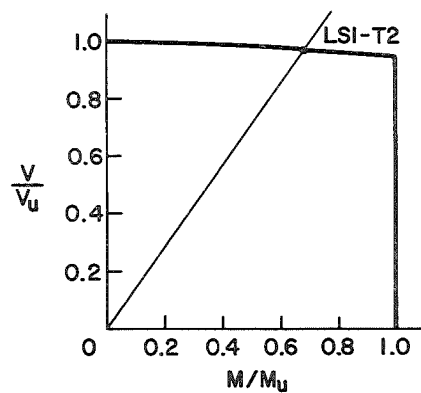


Fig. 12. Schematic Interaction Curves

328.10



328.10

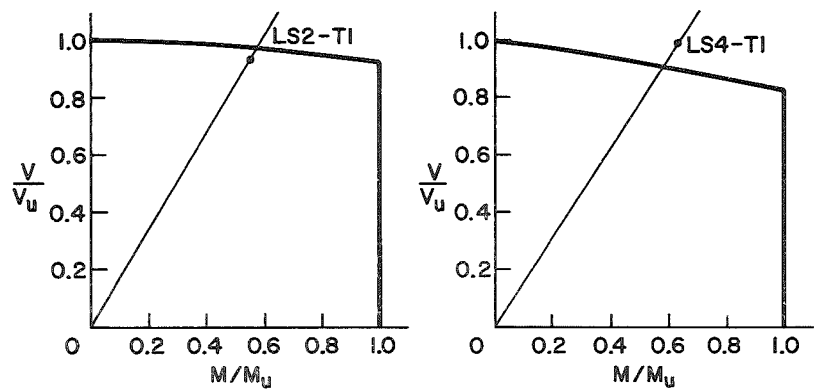
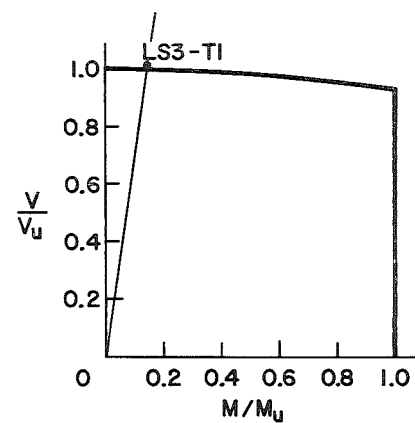


Fig. 13 Interaction Curves and Test Results of
LS1-T2, LS2-T2 & LS4-T1

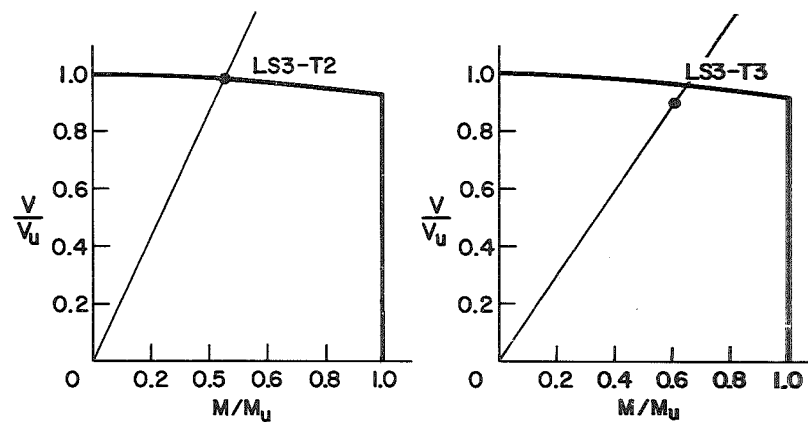
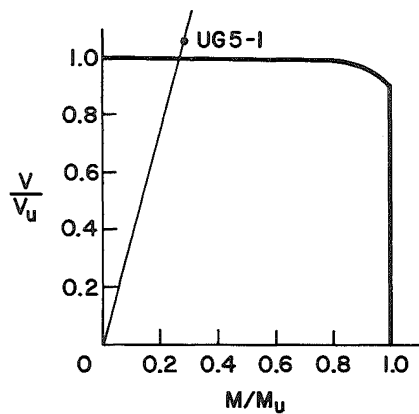


Fig. 14 Interaction Curves and Test Results of LS3-Series

328.10



328.10

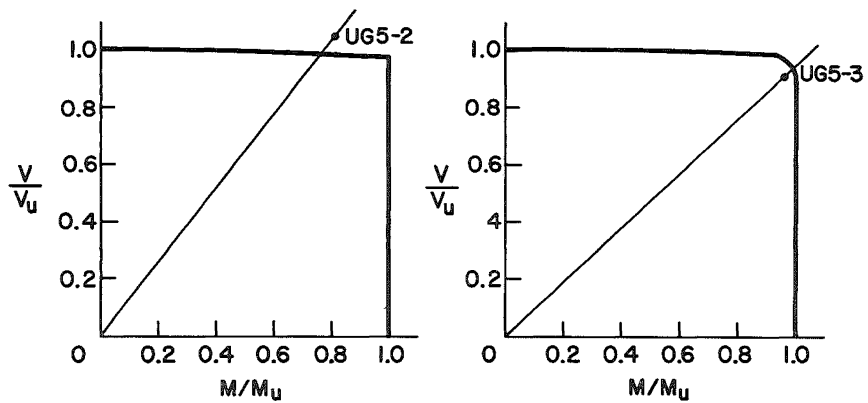
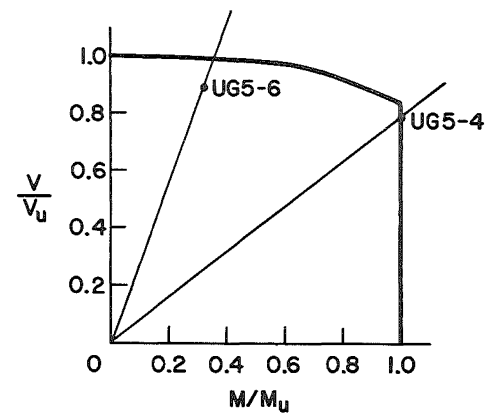


Fig. 15 Interaction Curves and Test Results of UG5.1, UG5.2 & UG5.3

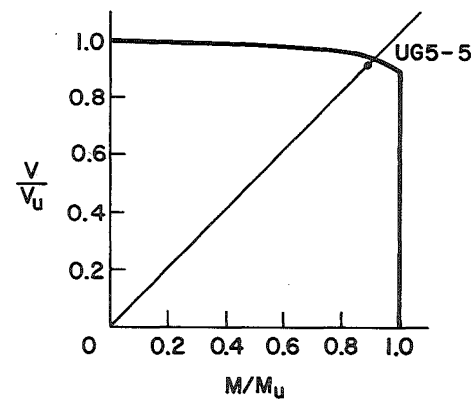


Fig. 16 Interaction Curves and Test Results of UG5.4, UG5.5 & UG5.6

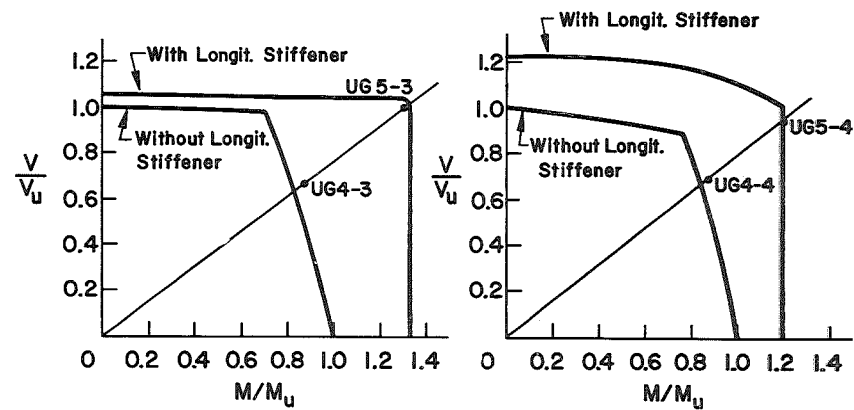
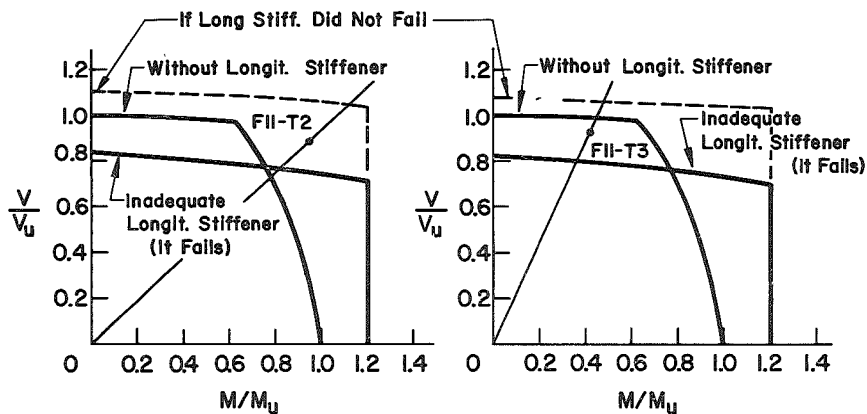
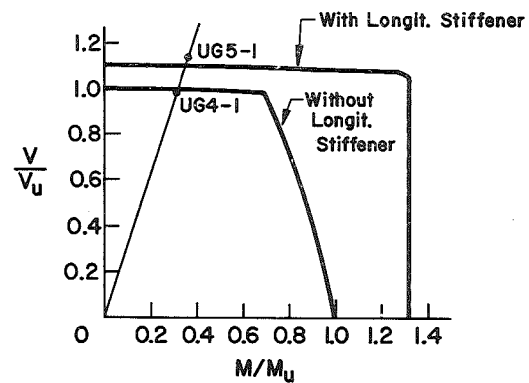
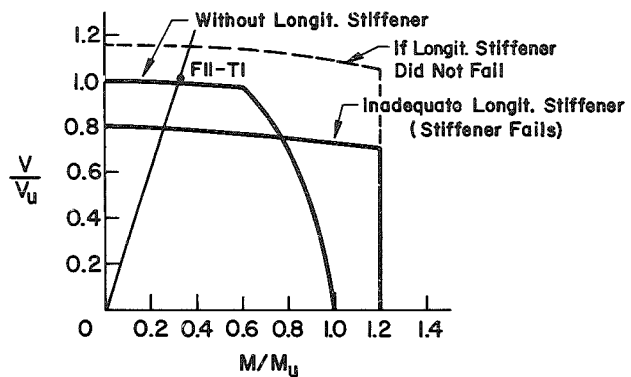


Fig. 17 Interaction Curves and Test Results of F11-Series

Fig. 18 Comparison of Panels With and Without Longitudinal Stiffeners - UG4 and UG5 Series